A Self-Trapping, Bipolar Viologen Bromide Electrolyte for Aqueous Redox Flow Batteries

Wenda Wu,[a] Jian Luo,[a] Fang Wang,[a] Bing Yuan,[b] T. Leo Liu[a,*]

a. Department of Chemistry and Biochemistry, Utah State University, Logan, UT, 84322, USA

b. State Key Laboratory Base of Eco-chemical Engineering, College of Chemistry and Molecular Engineering, Qingdao University of Science and Technology, Qingdao 266042, China

* Corresponding author: leo.liu@usu.edu, liugrouppub@gmail.com

TOC Figure

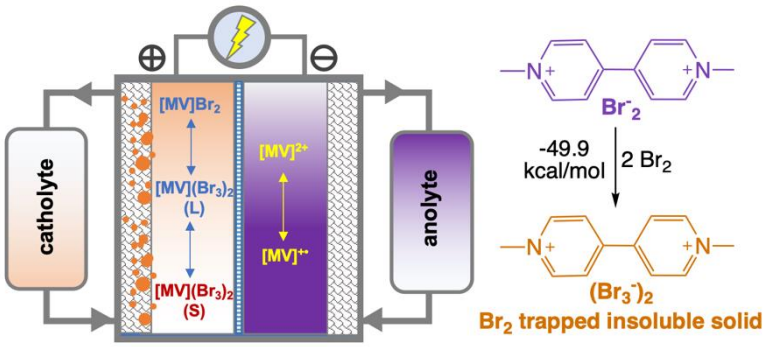

Keywords: Energy storage • redox flow batteries • viologen • bromine • redox active molecules

Abstract: Aqueous organic redox flow batteries (AORFBs) have become increasing attractive for scalable energy storage. However, it remains challenging to develop high voltage, powerful AORFBs because of the lack of catholytes with high redox potential. Herein, we report methyl viologen dibromide (**[MV]Br$_2$**) as a facile self-trapping, bipolar redox electrolyte material for pH neutral redox flow battery applications. The formation of the **[MV](Br$_3$)$_2$** complex was computationally predicted and experimentally confirmed. The low solubility **[MV](Br$_3$)$_2$** complex in the catholyte during the battery charge process not only mitigates the crossover of charged tribromide species (Br_3^-) and addresses the toxicity concern of volatile bromine simultaneously. A 1.53 V bipolar MV/Br AORFB delivered outstanding battery performance at pH neutral conditions, specifically, 100% total capacity retention, 133 mW/cm^2 power density, and 60% energy efficiency at 40 mA/cm^2.

In last decades, the development of environmentally friendly renewable energy resources has grown rapidly to achieve sustainable society. To efficiently utilize the intermittent energies such as sunshine and wind, advanced energy storage technologies are highly demanded.[1-3]

Redox flow batteries (RFBs, Scheme 1A) are favorably attractive for scalable and dispatchable energy storage by their advantages of decoupled energy and power, high current and power performance, non-flammable and low cost aqueous supporting electrolytes.[1-3] Traditional aqueous inorganic RFBs (AIRFBs) employing inorganic redox active compounds including metal salts and halides as energy storage materials have received massive studies.[4] However, materials challenges of AIRFBs including expensive active materials, corrosive electrolytes, electrolyte crossover, limited tunability, and side-reactions such as hydrogen evolution prevent their wide spread implementation and acceptance by industries.[1-2] To achieve economic and environmentally benign energy storage, tunable and sustainable redox active organic electrolyte materials[5-15] have been developed for RFB applications in recent years.[1-3]

We and other groups have demonstrated that viologen molecules, because of outstanding stability and high charge capacities, are privileged anolyte materials for pH neutral aqueous organic redox flow batteries.[2] Viologen compounds have been paired with TEMPO,[6-7] ferrocene,[8, 16-17] ferrocyanide,[18] and iodide,[19] for pH neutral AORFBs which delivered reliable current performance and superior cycling stability. Nevertheless, owing to the low redox potential of iodide ($E_{1/2}(I_3^-/I^-)$ = 0.57 V vs NHE), ferrocene ($E_{1/2}(FcNCl^{+/0})$ = 0.61 V, vs NHE), and ferrocyanide ($E_{1/2}([Fe(CN)_6]^{3-/4-}$) = 0.39 V vs NHE), these corresponding AORFBs could only deliver 0.82 - 1.06 V battery voltage. It is desired to develop high voltage AORFBs to boost energy and power densities simultaneously. Although viologen compounds have been paired with TEMPO compounds to achieve higher battery voltages, complicate synthesis, high cost and limited stability of TEMPO derivatives limited their practical development.[20] We recently reported a high voltage AORFB by pairing a sulfonate functionalized viologen compound, 1,1'-di(3-sulfonatopropyl)-4,4'-bipyridinium, $(SPr)_2V$, with a low cost bromide catholyte (NH_4Br).[20] In the $(SPr)_2V$/Br AORFB, however, the cycling stability was hindered by the crossover and volatilization of the tribromide species (Br_3^-).

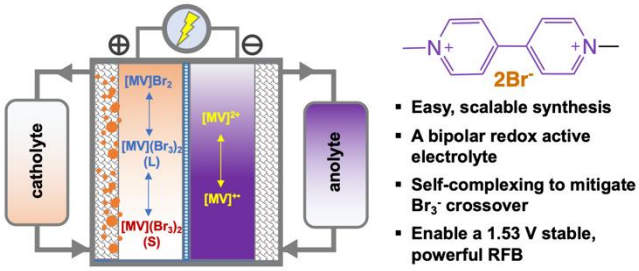

Scheme 1. (A) A schematic illustration of the bipolar MV/Br AORFB; and (B) Molecular structure of **[MV]Br2** and a highlight of its technical merits for flow battery applications.

To address the crossover and volatilization issues of bromine species, quaternary ammonium bromides were applied as complex reagents to trap the Br_3^- by complexation (typically forming a new liquid or solid phase) in battery studies.[21-22] Viologen molecules are di-pyridinium salts and are analogous to quaternary ammonium salts. Thus, we hypothesized that viologen molecules could stabilize the Br_3^- anion and might be capable to work as a redox active "self-trapping" reagent for viologen/Br AORFBs (equations 1-3). In the anolyte side, viologen is charged to its radical state for electron storage. In the catholyte side, the Br_3^- species generated in the charge process is expected to be trapped by the viologen cation to form a viologen-bromine complex, e.g. **[MV(Br$_3$)$_2$]** in the case of methyl viologen cations (MV^{2+}). In addition, the bipolar nature of **[MV]Br$_2$** will allow the use of a low-cost porous separator instead of using an expensive ion exchange membrane as reported in the previous studies. Our results revealed that **[MV]Br$_2$** can complex with Br_2 to form poorly soluble **[MV](Br$_3$)$_2$** to mitigate the crossover of the tribromide species (Br_3^-) during flow battery operation. A 1.53 V bipolar MV/Br AORFB (10.2 Wh/L) demonstrated outstanding battery performance, including high stability (100% capacity retention for 100 cycles) and high-power density (up to 133 mW/cm^2).

$$\text{Anolyte: } MV^{2+} + e^- \rightleftarrows MV^{\cdot+} \qquad (1)$$

$$\text{Catholyte: } 6Br^- - 4e^- \rightleftarrows 2Br_3^- + MV^{2+} \rightleftarrows [MV](Br_3)_2 \downarrow \qquad (2)$$

$$\text{Full cell: } 2MV^{2+} + 6Br^- \rightleftarrows MV^{\cdot+} + [MV](Br_3)_2 \downarrow \qquad (3)$$

Firstly, we proposed two reactions that the **[MV]**$^{2+}$ cation would complex with Br_3^- anions (equations 4 and 5). Then, Density Functional Theory (DFT) computational studies at the M06-2x/6-31+G* level with the SMD solvation model were conducted to find out the most possible complexing reactions by calculating thermal free energies of reactants and products. Figures 1A-1C display the optimized structures of **[MV]Br$_2$**, and its Br_2-complexing products, **[MV]Br$_3$Br** and **[MV](Br$_3$)$_2$**. Br_3^- (or Br^-) anions are placed at each side the bis-pyridinium moiety. Consistent with the ionic bonding interaction, Br^- anions are positioned about 3.30 Å from the N atoms of the **[MV]**$^{2+}$ cation in **[MV]Br$_2$**. After the complexing of Br_2, the distance between Br_3^- and N slightly increases to about 3.36 Å in **[MV]Br$_3$Br** and **[MV](Br$_3$)$_2$**, reflecting the dispersed electron density of Br_3^- anion and a weaker electrostatic interaction with the pyridinium moiety. According to DFT results, one **[MV]Br$_2$** molecule can bind two Br_3^- anions with a down-hill free energy of -49.42 kcal/mol energy, which is two times more favorable than binding with one Br_3^- (equations 4 and 5; see the SI for more computational

details).

$$[MV]Br_2 + Br_2 \rightleftarrows [MV]Br_3Br \qquad \triangle G = -23.84 \text{ kcal/mol (4)}$$

$$[MV]Br_2 + 2Br_2 \rightleftarrows [MV](Br_3)_2 \qquad \triangle G = -49.42 \text{ kcal/mol (5)}$$

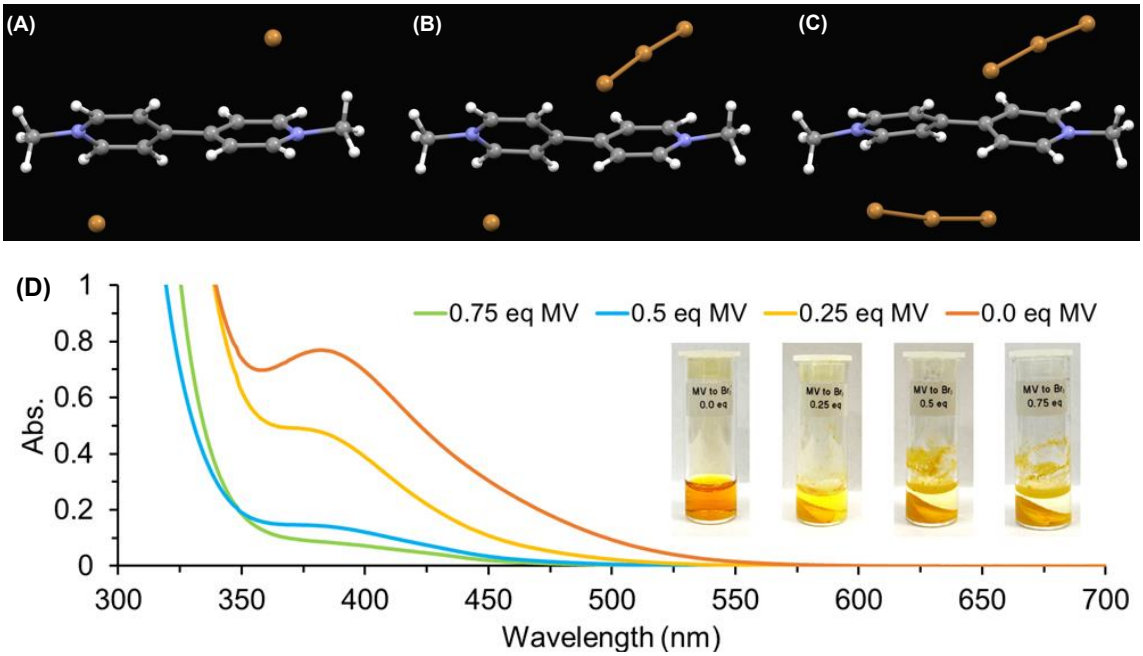

Figure 1. Optimized structures of (A) **[MV]Br$_2$**, (B) **[MV]Br$_3$Br**, and (C) **[MV](Br$_3$)$_2$**, and (D) UV-Vis spectrum for the $NaBr_3$ titration experiment with **[MV]Br$_2$**. All titrated samples have diluted five times before test. The fresh $NaBr_3$ sample (0.0 eq. **[MV]Br$_2$**) was diluted 40 times from 0.25 M for measurement. Inserted photos are the centrifuged samples from the titration experiment before dilution for UV-Vis test to show the color change and the formation of precipitate.

After confirming the hypothesis computationally, the bipolar **[MV]Br$_2$** compound was conveniently prepared using 4,4'-bipyridine and bromoacetic acid in a yield of 95 % at the scale of more than 20 g. Then, the complexing efficiency of the **[MV]**$^{2+}$ dication with Br_3^- were studied by UV-Vis through a titration experiment. As it is depicted in the photos in Figure 1D, a series of 0.25 M $NaBr_3$ solutions were titrated by **[MV]Br$_2$** with an increasing concentration gradient and the free Br_3^- concentration was determined by a calibration curve. As shown in the inserted figure in Figure 1D, after 0.25 eq of **[MV]Br$_2$** was added, the free Br_3^- concentration decreased dramatically from 0.25 M to 0.019 M and it further decreased to 0.0047 M if 0.5 eq MV^{2+} was added. With 0.75 eq of **[MV]**$^{2+}$, Br_3^- diagnostic absorbance peak at 386 nm became too weak to be observed. The solubility of **[MV](Br$_3$)$_2$** was then measured by ^{1}H-NMR as low as 20 mM in deionized water as shown in Figure S3. The high sedimentation efficiency of **[MV]**$^{2+}$ with Br_3^- and the low solubility of **[MV](Br$_3$)$_2$** precipitate credibly suggest a low possibility of Br_3^- crossover in the battery cycling process of a bipolar

MV/Br AORFB, which would be a great enhancement for the battery's long term stability. It should be noted that the formation of solid **[MV](Br$_3$)$_2$** phase is also beneficial to mitigate the toxic concern of volatile Br_2.

We proceeded to study the electrochemical properties of the bipolar compound, **[MV]Br$_2$**. Electrochemical properties of **[MV]Br$_2$** in a NaBr supporting electrolyte were studied by cyclic voltammetry (CV) and linear sweep voltammetry (LSV) with rotating disc electrode (RDE). As shown in Figure 2A, both **[MV]$^{2+}$** cation and bromide anion exhibited reversible CV signals in aqueous solution with $E_{1/2}$(MV) = -0.45 V and $E_{1/2}$(Br) = 1.08 V (vs NHE), giving a 1.53 V battery voltage for the MV/Br AORFB. Scan rate dependence studies revealed that the separation of the cathodic and anodic waves of **[MV]$^{2+}$** remained constantly ca. 57 mV (Figure 2B), indicative of a fast electron transfer rate. Then the electron-transfer rate constant (k^0) of **[MV]$^{2+}$** in the NaBr supporting electrolyte was estimated as 0.35 cm/s by Nicholson's method (see the SI for detail). The diffusion coefficient (D) of **[MV]$^{2+}$** was calculated as 5.02 x 10^{-6} cm^2/s by the Levich equation using the RDE data (Figures 3C and 3D).

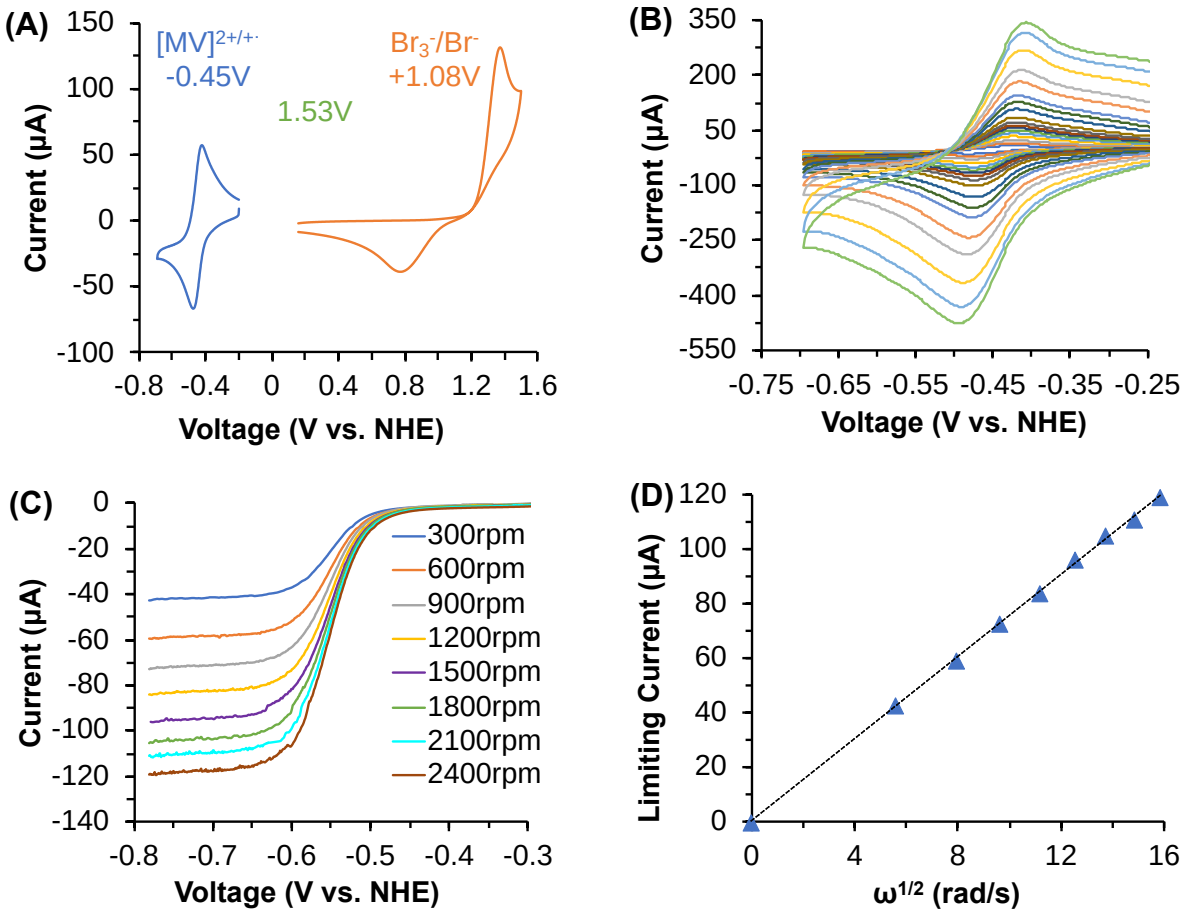

Figure 2. (A) Cyclic voltammograms of **[MV]Br$_2$** with **[MV]$^{2+}$**/**[MV]$^{+\cdot}$** at -0.45 V and Br^-/Br_3^- at 1.08 V. (B) Cyclic voltammograms of MV (scan rates from 5 to 2500 mV/s). Experiment conditions for (A) and (B): 4.0 mM **[MV]Br$_2$** in 0.5 M NaBr aqueous electrolyte, 100 mV/s scan rate, glassy carbon working electrode, carbon counter electrode, and Ag/AgCl reference

electrode. (C) LSV scans with using a glassy carbon rotating working electrode for the reduction of **[MV]Br$_2$**. Experiment conditions: 1.0 mM **[MV]Br$_2$** in 0.5 M NaBr (D) Levich plot based on the LSV data.

The "self-complexing" bipolar **[MV]Br$_2$** AORFB was demonstrated at an energy density of 10.2 Wh/L using 0.5 M **[MV]Br$_2$** in 2.0 M NaCl supporting electrolyte at pH = 7.0 as both anolyte and catholyte while a Daramic porous membrane was applied as a separator. This AORFB was charged and discharged between 1.8 and 0.2 V. As shown in Figures 3A and 3B, the **[MV]Br$_2$** AORFB was able to operate under 40, 60, 80, and 100 mA/cm^2. This battery delivered an average columbic efficiency of 96.5% at each current density. An energy efficiency and a voltage efficiency were obtained at 60% at an operational current density of 40 mA/cm^2. Interestingly, the solid phase formation did not affect the current performance of the battery as it was cycled up to 100 mA/cm^2 with an energy efficiency of 50%. It was observed that the charged catholyte **[MV](Br$_3$)$_2$** was primarily deposited on the porous carbon electrode while it also partially suspended in the solution phase (see Figure 1A). It is believed both solid and solution (20 mM) phases of **[MV](Br$_3$)$_2$** could proceed with the discharge step. Alternatively, the solid phase can go back to the solution phase and then undergo discharge. The long-term cycling performance of the **[MV]Br$_2$** AORFB was studied by 100 charge/discharge extended cycles under 60 mA/cm^2. As shown in Figure 3D, the **[MV]Br$_2$** AORFB displayed impressive cycling performance, specifically, after 100 charge/discharge cycles, 100% total capacity retention or 100% capacity retention per cycle with an average energy efficiency of 55.82% and a coulombic efficiency of 97.70%. As shown in Figure S1, the charge/discharge curves of the 1st and 100th cycle were nearly overlapped. The polarization curve of the MV/Br AORFB was collected under 100% state of charge (SOC) as illustrated in Figure 3C. A peak power density of 132.7 mW/cm^2 was recorded at an open circuit voltage (OCV) of 1.37 V. The chemical stability of **[MV]Br$_2$** during the battery cycling process was confirmed by post-cycling analysis using ^{1}H-NMR (Figure S2). After mixing the catholyte and anolyte at 100% state of discharge, no new peak was observed in the ^{1}H-NMR spectrum, which indicates that the $MV^{+\cdot}$ radical cation did not undergo chemical degradation such as the bromination side-reaction.

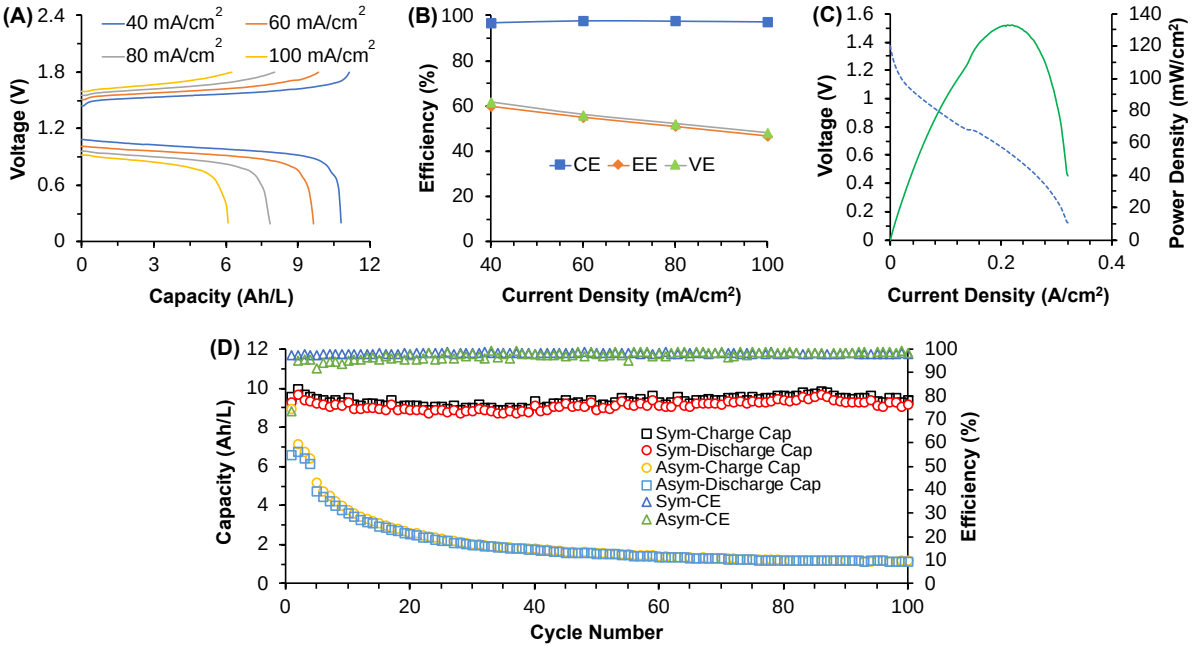

Figure 3. Flow battery studies of **[MV]Br2**. (A) Representative charge and discharge plots at current densities from 40 to 100 mA/cm^2. (B) Plots of average Coulombic efficiency (CE), energy efficiency (EE), and voltage efficiency (VE) at different operational current densities. (C) Polarization (dash) and power density (solid) curves collected at 100% SOC. (D) Extended 100 cycle data of the same symmetric MV/Br AORFB for power density test in graph C and a comparison with an asymmetric MV/Br AORFB.

As a comparison, an asymmetric MV/Br AORFB with 0.5 M **[MV]Br2** in 2.0 M NaCl as anolyte and 1.25 M NaBr in 1.25 M NaCl as catholyte was tested under the same condition. In a stark contrast, quick capacity fading (> 50%) was observed within first 10 cycles without **[MV]**$^{2+}$ as the Br_3^- trapper at the catholyte side (Figure 3D). After 100 cycle, only a capacity of 1.2 Ah/L was retained, representing ca. 16% capacity retention. The coulombic efficiency of the asymmetric MV/Br RFB was firstly obtained as ca. 93% at the beginning and slowly improved for later cycles. The quick capacity decay of the asymmetric flow battery suggests strong crossover of active materials. The phenomenon of the severe crossover of Br_3^- in the absence of **[MV]**$^{2+}$ was confirmed by a post-cell analysis.

In summary, we mechanistically designed a novel "self-trapping" MV/Br AORFB using a bipolar electrolyte compound, **[MV]Br2**, as both anolyte and catholyte at pH neutral conditions. The formation of **[MV](Br3)2** complex was proved computationally and experimentally to be an efficient bromine complexing strategy. In the catholyte side of symmetric MV/Br AORFB, MV could significantly avoid the bromine species crossover which results in stable cycling performance comparing to the asymmetric MV/Br AORFB. The demonstrated symmetric MV/Br AORFB delivered nearly 100% capacity retention in 100 charge/discharge cycles and a power density of 133 mW/cm^2. The reliable cycling performance and low cost of the pH

neutral bipolar **[MV]Br$_2$** AORFBs makes it as a promising solution to large scale energy storage. The newly discovered self-complexing strategy of viologen cations reported herein will inspire the development of new viologen molecules and other molecular designs for bipolar RFBs.

Supporting Information contains experimental details and additional figures and tables. Supporting Information is available online or from the author.

Acknowledgements We thank National Science Foundation Career Award (Grant No. 1847674) and faculty startup funds from Utah State University for supporting our flow battery project. Bing Yuan acknowledge s the China CSC Study Abroad program for supporting her study at USU.

References:

1. Winsberg, J.; Hagemann, T.; Janoschka, T.; Hager, M. D.; Schubert, U. S., Redox-Flow Batteries: From Metals to Organic Redox-Active Materials. *Angew. Chem. Int. Ed.* **2016,** *56*, 686-711.
2. Luo, J.; Hu, B.; Hu, M.; Zhao, Y.; Liu, T. L., Status and Prospects of Organic Redox Flow Batteries towards Sustainable Energy Storage. *ACS Energy Lett.* **2019,** *4*, 2220-2236.
3. Wei, X.; Pan, W.; Duan, W.; Hollas, A.; Yang, Z.; Li, B.; Nie, Z.; Liu, J.; Reed, D.; Wang, W.; Sprenkle, V., Materials and Systems for Organic Redox Flow Batteries: Status and Challenges. *ACS Energy Lett.* **2017**, 2187-2204.
4. Hu, B.; Luo, J.; Debruler, C.; Hu, M.; Wu, W.; Liu, T. L., In *"Redox-Active Inorganic Materials for Redox Flow Batteries", Ency. Inorg. Bioinorg. Chem.* , 2019; pp 1-25.
5. Janoschka, T.; Martin, N.; Martin, U.; Friebe, C.; Morgenstern, S.; Hiller, H.; Hager, M. D.; Schubert, U. S., An Aqueous, Polymer-based Redox-Flow Battery Using Non-corrosive, Safe, and Low-cost Materials. *Nature* **2015,** *527* (7576), 78-81.
6. Liu, T.; Wei, X.; Nie, Z.; Sprenkle, V.; Wang, W., A Total Organic Aqueous Redox Flow Battery Employing a Low Cost and Sustainable Methyl Viologen Anolyte and 4-HO-TEMPO Catholyte. *Adv. Energy Mater.* **2016,** *6* (3), 1501449.
7. Janoschka, T.; Martin, N.; Hager, M. D.; Schubert, U. S., An Aqueous Redox-Flow Battery with High Capacity and Power: The TEMPTMA/MV System. *Angew. Chem. Int. Ed.* **2016,** *55* (46), 14427-14430.
8. Hu, B.; DeBruler, C.; Rhodes, Z.; Liu, T. L., Long-Cycling Aqueous Organic Redox Flow Battery (AORFB) toward Sustainable and Safe Energy Storage. *J. Am. Chem. Soc.* **2017,** *139* (3), 1207-1214.
9. Hu, B.; Luo, J.; Hu, M.; Yuan, B.; Liu, T. L., A pH Neutral, Metal Free Aqueous Organic Redox Flow Battery Employing an Ammonium Anthraquinone Anolyte. *Angew. Chem. Int. Ed.* **2019,** *58* (ja), 2-11.
10. Hollas, A.; Wei, X.; Murugesan, V.; Nie, Z.; Li, B.; Reed, D.; Liu, J.; Sprenkle, V.; Wang, W., A Biomimetic High-capacity Phenazine-based Anolyte for Aqueous Organic Redox Flow Batteries. *Nat. Energy* **2018,** *3* (6), 508-514.
11. Chen, Y.; Zhou, M.; Xia, Y.; Wang, X.; Liu, Y.; Yao, Y.; Zhang, H.; Li, Y.; Lu, S.; Qin, W.;

Wu, X.; Wang, Q., A Stable and High-Capacity Redox Targeting-Based Electrolyte for Aqueous Flow Batteries. *Joule* **2019,** *3* (9), 2255-2267.
12. Ji, Y.; Goulet, M.-A.; Pollack, D. A.; Kwabi, D. G.; Jin, S.; De Porcellinis, D.; Kerr, E. F.; Gordon, R. G.; Aziz, M. J., A Phosphonate-Functionalized Quinone Redox Flow Battery at Near-Neutral pH with Record Capacity Retention Rate. *Adv. Energy Mater.* **2019,** *9* (12), 1900039.
13. Yang, C.; Nikiforidis, G.; Park, J. Y.; Choi, J.; Luo, Y.; Zhang, L.; Wang, S.-C.; Chan, Y.-T.; Lim, J.; Hou, Z.; Baik, M.-H.; Lee, Y.; Byon, H. R., Designing Redox-Stable Cobalt–Polypyridyl Complexes for Redox Flow Batteries: Spin-Crossover Delocalizes Excess Charge. *Adv. Energy Mater.* **2018,** *8*, 170289.
14. Zhang, C.; Niu, Z.; Peng, S.; Ding, Y.; Zhang, L.; Guo, X.; Zhao, Y.; Yu, G., Phenothiazine-Based Organic Catholyte for High-Capacity and Long-Life Aqueous Redox Flow Batteries. *Adv. Mater.* **2019,** *31* (24), 1901052.
15. Zhang, J.; Yang, Z.; Shkrob, I. A.; Assary, R. S.; Tung, S. o.; Silcox, B.; Duan, W.; Zhang, J.; Su, C. C.; Hu, B.; Pan, B.; Liao, C.; Zhang, Z.; Wang, W.; Curtiss, L. A.; Thompson, L. T.; Wei, X.; Zhang, L., Annulated Dialkoxybenzenes as Catholyte Materials for Non-aqueous Redox Flow Batteries: Achieving High Chemical Stability through Bicyclic Substitution. *Adv. Energy Mater.* **2017,** *7*, 1701272.
16. Beh, E. S.; De Porcellinis, D.; Gracia, R. L.; Xia, K. T.; Gordon, R. G.; Aziz, M. J., A Neutral pH Aqueous Organic–Organometallic Redox Flow Battery with Extremely High Capacity Retention. *ACS Energy Lett.* **2017,** *2*, 639-644.
17. DeBruler, C.; Hu, B.; Moss, J.; Liu, X.; Luo, J.; Sun, Y.; Liu, T. L., Designer Two-Electron Storage Viologen Anolyte Materials for Neutral Aqueous Organic Redox Flow Batteries. *Chem* **2017,** *3*, 1-18.
18. Luo, J.; Hu, B.; Debruler, C.; Bi, Y.; Zhao, Y.; Yuan, B.; Hu, M.; Wu, W.; Liu, T. L., Unprecedented Capacity and Stability of Ammonium Ferrocyanide Catholyte in pH Neutral Aqueous Redox Flow Batteries. *Joule* **2019,** *3*, 1-15.
19. DeBruler, C.; Hu, B.; Moss, J.; Luo, J.; Liu, T. L., A Sulfonate-Functionalized Viologen Enabling Neutral Cation Exchange, Aqueous Organic Redox Flow Batteries toward Renewable Energy Storage. *ACS Energy Lett.* **2018,** *3*, 663-668.
20. Luo, J.; Wu, W.; Debruler, C.; Hu, B.; Hu, M.; Liu, T. L., A 1.51 V pH neutral redox flow battery towards scalable energy storage. *J. Mater. Chem. A* **2019,** *7* (15), 9130-9136.
21. Mastragostino, M.; Valcher, S., Polymeric salt as bromine complexing agent in a Zn-Br2 model battery. *Electrochim. Acta* **1983,** *28* (4), 501-505.
22. Bauer, G.; Drobits, J.; Fabjan, C.; Mikosch, H.; Schuster, P., Raman spectroscopic study of the bromine storing complex phase in a zinc-flow battery. *J. Electroanal. Chem.* **1997,** *427* (1), 123-128.